have been expressed in terms of four autocorrelated reduced Cartesian power densities. The Cartesian form of the spectral densities leads to expressions for the correlation times, and the correlation times have a simple physical interpretation.

The Cartesian correlation functions describe the reorientation of geometrical constructs having the shape of d orbitals. Thus, τ_{xx}, τ_{yy}, and τ_{zz} are the correlation times for the motion of a d_0 structure fixed along the x, y, and z axes, respectively, while τ_{xy} and τ_{xx-yy} are the correlation times of a clover leaf structure of the d_{xy} and d_{xx-yy} form.[20] As with d orbitals, τ_{xx-yy} is linearly dependent upon τ_{xx}, τ_{yy}, and τ_{zz} and so a degree of arbitrariness in our final choice of basis must be recognized. Under axial symmetry about the z axis, τ_{xy} and τ_{xx-yy} are equal as are τ_{xx} and τ_{yy}. Rotational correlation functions exist for xz and yz constructs, but for the AX_2 spin system discussed in this paper it is not possible to determine these specific power densities experimentally from the spin-relaxation data because of the symmetry and orientation of the spin system.

When a rigid molecule rotates in accord with the small step diffusion model, the Cartesian correlation functions (either in the form of $\hat{J}$'s or τ's) may be directly related to the rotational diffusion tensor. The only case treated here is that where the principal axes of the molecular diffusion tensor are coincident with the symmetry axes of the AX_2 spin system. Other spatial relationships could be derived as needed. In Cartesian form the power densities are free of molecular structural parameters and relate directly to the rotational diffusion tensor. If the molecule is rigid and conforms to the diffusion equation, the four otherwise linearly independent correlation times can be expressed in only three terms (τ_{xx}, τ_{yy}, and τ_{zz} are a convenient subset), leaving the fourth dipolar power density available for setting one of the structural parameters (e.g., the XAX' angle). Symmetric top and spherical top conditions reduce the number of correlation functions to two and one, respectively.

A direct relationship between τ's and the D's is not known in cases where the rotational dynamics are not diffusional. For molecules undergoing extended free precession or large angle jumps, or for flexible molecules, there is no simple relationship between a correlation time a diffusion coefficient. Likewise, more than three correlation times are necessary to define the dynamics completely as has been shown by Lynden-Bell.[21] Nonetheless, because the Cartesian correlation times or power densities are model independent, they continue to be an appropriate parameter set to characterize the motions important in spin relaxation. The four experimental correlation times provide a stiff test of alternative theoretical models of molecular motion. When the molecular motion has important frequency components in the relevant NMR frequency range, no more powerful spectroscopic method exists for characterizing the anisotropy of motion affecting the coupled spins.

Acknowledgment. The Utah group is grateful to the National Institute of Health, Grant No. GM08521-24, for partial support of ths research. G.T.E. is supported in part by a grant from the National Science Foundation and wishes to express his gratitude for the hospitality and guidance of Professor Daniel Kivelson during G.T.E's sabbatical leave at UCLA.

(20) Please note that a d_0 construct arises from the zeroth projection of the second-order Legendre polynomial, $\langle P_2(e_i(0)\cdot e_i(t))\rangle$, where e_i in the dot product is the unit vector pointing along the $i(x,y,z)$ axis. The d_{xy} construct, while not a zeroth projection of P_2 is no less important in a complete description of the molecular motion and may also be expressed as a dot product of unit vectors, i.e., $2J_{xy} = \int_0^\infty dt\,[\langle P_1(e_x\cdot e_y(t))P_1(e_y\cdot e_x(t))\rangle + \langle P_1(e_y\cdot e_y(t))P_1(e_x\cdot e_x(t))\rangle]$. At time zero the first term is zero and likely never grows very large. The second term, however, starts at unity, but will rapidly, compared with a P_2 function, drop to zero because if the motion does not dephase the dot product $e_x e_x(t)$ it must of necessity dephase the dot product in y and vice versa.

(21) Lynden-Bell, R. M. *Chem. Phys. Lett.* **1980**, *70*, 477.

Rotational Dynamics of Flexible Alkanes. An NMR Coupled Relaxation and a Brownian Dynamics Study[1]

Mark S. Brown,[†] David M. Grant,*[†] W. J. Horton,[†] Charles L. Mayne,[†] and Glenn T. Evans[‡]

Contribution from the Departments of Chemistry, University of Utah, Salt Lake City, Utah 84112, and Oregon State University, Corvallis, Oregon 97331. *Received January 17, 1985*

Abstract: The selectively labeled nonanes $C_4D_9{}^{13}CH_2C_4D_9$ and $C_7D_{15}{}^{13}CH_2CD_3$ and the heneicosane $C_{10}D_{21}{}^{13}CH_2C_{10}D_{21}$ have been synthesized and the spin–lattice relaxations of the isolated $^{13}CH_2$ groups studied by carbon-13 NMR coupled relaxation methods. Selective and nonselective π pulses were applied to the carbon and proton transitions of these AX_2 spin systems and partially relaxed carbon-13 spectra were obtained for various evolution periods after the pulse. Experiments were performed on the nonanes at 233, 273, 313, and 353 K, and on the heneicosane at 313, 353, and 393 K. The data are fitted using the Redfield formalism for NMR dipolar relaxation in terms of four dipolar spectral densities J_{CH}, J_{HCH}, J_{CHH}, and J_{HH}. These four spectral densities are transformed to a reduced Cartesian basis as described in the previous paper by Fuson et al. to give model independent reorientational correlation times τ_{xx}, τ_{yy}, τ_{zz}, and τ_{xy}. The correlation times are compared with results calculated from computer simulations utilizing a Brownian dynamics algorithm. Generally, the results indicate that the motion at each segment of the chain has local prolate symmetric top character and that the correlation times indicate greater motional anisotropy at the middle of a chain than the ends. There is good agreement between the experimental and theoretical correlation times, both in terms of absolute values and in degree of anisotropy.

I. Introduction

Nuclear magnetic resonance (NMR) relaxation experiments are widely used to investigate the rotational dynamics and structure of molecules in solution. The most commonly performed experiments (e.g., inversion recovery, NOE) are generally interpreted in terms of the longitudinal (or spin–lattice) relaxation time T_1 and the transverse (or spin–spin) relaxation time T_2. These time constants are used in the Bloch equations[2-4] to describe the relaxation of an isolated spin $^1/_2$ nucleus. In more complicated spin

[†] University of Utah.
[‡] Camille and Henry Dreyfus Teacher-Scholar; Oregon State University.

0002-7863/85/1507-6698$01.50/0

systems, the magnetization must be described by several exponential functions of time, and single T_1 and T_2 time constants are inadequate to explain the relaxation.[5,6] Analysis of coupled spin relaxation to obtain spectral densities and relaxation rates can be an involved procedure in the AX_2 spin systems considered here. However, in support of this procedure, previous studies on isotropic solution[7-15] and nematic phases[16-22] have shown that NMR relaxation in multispin systems is indeed a very sensitive method for probing certain structural features of a molecule as well as its rotational dynamics in solution. Here, the coupled relaxation technique is used to investigate the dynamics of overall and internal rotations of selected methylene groups in nonane and heneicosane in solutions over a range of temperatures.

Recently, there has been a significant amount of activity directed toward the understanding of the dynamics of flexible chain molecules in liquids.[23-49] The rotational and torsional motions affect intramolecular reaction rates as well as spectral and transport properties.[49] Despite the central importance of understanding how alkanes change shape in normal fluids at room temperatures, there is a serious lack of experimental data suitable for careful and meaningful comparisons to theory. Several experiments have been conducted on alkanes in condensed liquids, and these experiments are capable, at least in principle, of measuring torsional and rotational dynamics. Experiments such as dielectric relaxation[50] and depolarized light scattering[51] detect the collective dynamics of the whole molecule instead of just a single molecular segment. Furthermore, in the interpretation of depolarized light scattering from flexible polyatomic molecules, an ambiguity exists as a molecular expression for the polarizability tensor is unknown.[52] Spin-relaxation is free of both of these problems because it depends upon a molecular segment's properties associated with a precisely known dynamic variable (in this case the magnetic dipole–dipole interaction).

Medium-sized alkanes have been studied previously using NMR.[53-55] This NMR work dealt primarily with a single T_1 for each methylene group along the chain backbone. Modeling the relaxation with only one T_1 can provide only one effective rotational correlation time. These effective correlation times correspond to an imprecise dynamical variable, not readily compared with theory, and imply that the methylene group rotates as a rigid sphere. In the present study, the coupled relaxation data acquired on several alkanes will be fitted using previously defined notation[7-9,15] and the Redfield formalism[56,57] to deduce four dipolar spectral densities: J_{CH}, J_{HH}, J_{CHH}, and J_{HCH}. Two of the power densities, J_{CHH} and J_{HCH}, are cross correlation terms and are difficult to interpret intuitively. Previous investigations using coupled relaxation methods[7-12] analyzed the spectral densities in light of a specific model for the dynamics (e.g., rotational diffusion) in order to obtain correlation times and diffusion coefficients. However, in the accompanying work,[1] the second-rank rotational correlation times (τ_{xx}, τ_{yy}, τ_{zz}, and τ_{xy}) were related directly to the power densities without specifying the dynamical model. Thus, at each specific position in a flexible molecule, these are the second-rank rotational correlation times. Furthermore, each of the four autocorrelation times can be interpreted in terms of a geometrical construct. It is these model-free correlation times that will serve as the data base in comparing and in evaluating Brownian dynamics simulations of chain motions in flexible molecules.

The specific systems studied here are the isotopically labeled *n*-nonanes $C_4D_9{}^{13}CH_2C_4D_9$ and $C_7D_{15}{}^{13}CH_2CD_3$ and the C_{21} chain, *n*-heneicosane ($C_{10}D_{21}{}^{13}CH_2C_{10}D_{21}$). These compounds were chosen for use in an NMR coupled relaxation experiment to investigate the effect of overall chain length (C_9 vs. C_{21}) and relative $^{13}CH_2$ position in the nonane chain (C-2 vs. C-5) on the relaxation times. Hydrogen nuclei (spin $^1/_2$) on the chain were replaced with low γ deuterium nuclei (spin 1) in order to spin-isolate the AX_2 (CH_2) groups. Because internal rotations and flexibility become more pronounced as the chain length increases, chains of moderate length were chosen. In the very short alkanes, such as butane, the molecule rotates nearly as a rigid body. Very long alkanes undergo slow overall rotation and so in order to observe a mixture of overall and internal rotations, molecules in the C_9 and C_{21} range were studied. Chains with an odd number of backbone atoms were selected so that a methylene exactly in

(1) Fuson, M. M.; Brown, M. S.; Grant, D. M.; Evans, G. T. *J. Am. Chem. Soc.*, preceding paper in this issue.
(2) Bloch, F. *Phys. Rev.* **1956**, *102*, 104.
(3) Bloch, F. *Phys. Rev.* **1957**, *105*, 1206.
(4) Wangsness, R. K.; Bloch, F. *Phys. Rev.* **1953**, *89*, 728.
(5) Werbelow, L. G.; Grant, D. M. *Adv. Magn. Reson.* **1977**, *9*, 189.
(6) Vold, R. L.; Vold, R. R. *Prog. Nucl. Magn. Reson. Spectrosc.* **1978**, *12*, 79.
(7) Mayne, C. L.; Alderman, D. W.; Grant, D. M. *J. Chem. Phys.* **1975**, *63*, 2514.
(8) Chenon, M. T.; Bernassau, J. M.; Mayne, C. L.; Grant, D. M. *J. Phys. Chem.* **1982**, *86*, 2733.
(9) Mayne, C. L.; Grant, D. M.; Alderman, D. W. *J. Chem. Phys.* **1976**, *65*, 1684.
(10) Fuson, M. M.; Prestegard, J. H. *J. Chem. Phys.* **1982**, *76*, 1539.
(11) Fuson, M. M.; Prestegard, J. H. *J. Am. Chem. Soc.* **1983**, *105*, 168.
(12) Fuson , M. M.; Prestegard, J. H. *Biochemistry* **1983**, *22*, 1311.
(13) Bovee, W. M. M. *Mol. Phys.* **1975**, *2*., 1673.
(14) Bodenhausen, G.; Szeverenyi, N. M.; Vold, R. L.; Vold, R. R. *J. Am. Chem. Soc.* **1978**, *100*, 6265.
(15) Brown, M. S.; Mayne, C. L.; Grant, D. M.; Chou, T. C.; Allred, E. L. *J. Phys. Chem.* **1984**, *88* 2708.
(16) Vold, R. R.; Vold, R. L. *J. Chem. Phys.* **1979**, *71*, 1508.
(17) Courtieu, J. M.; Fagerness, P. E.; Grant, D. M. *J. Chem. Phys.* **1977**, *65*, 1202.
(18) Courtieu, J. M.; Mayne, C. L.; Grant, D. M. *J. Chem. Phys.* **1977**, *66*, 2669.
(19) Werbelow, L. G.; Grant, D. M.; Black, E. P.; Courtieu, J. M. *J. Chem. Phys.* **1978**, *69*, 2407.
(20) Bernassau, J. M.; Black, E. P.; Grant, D. M. *J. Chem. Phys.* **1982**, *76*, 253.
(21) Courtieu, J.; Lai, N. T.; Mayne, C. L.; Bernassau, J. M.; Grant, D. M. *J. Chem. Phys.* **1982**, *76*, 257.
(22) Black, E. P. Bernassau, J. M.; Mayne, C. L.; Grant, D. M. *J. Chem. Phys.* **1982**, *76*, 265.
(23) Ryckaert, J. P.; Bellemans, A. *Chem. Phys. Lett.* **1975**, *30*, 123.
(24) Fixman, M. *J. Chem. Phys.* **1978**, *69*, 1527. Fixman, M.; Evans, G. T. *Ibid.* **1978**, *68*, 195.
(25) Fixman, M. *J. Chem. Phys.* **1978**, *69*, 1538.
(26) Helfand, E.; Wasserman, Z. R.; Weber, T. A. *J. Chem. Phys.* **1979**, *70*, 2016.
(27) Helfand, E.; Wasserman, Z. R.; Weber, T. A. *Macromolecules* **1980**, *13*, 526.
(28) Levy, R. M.; Karplus, M.; McCammon, J. A. *Chem. Phys. Lett.* **1979**, *65*, 4.
(29) Montgomery, J. A.; Chandler, D.; Berne, B. J. *J. Chem. Phys.* **1979**, *70*, 4056.
(30) Montgomery, J. A.; Holmgren, S. L.; Chandler, D. *J. Chem. Phys.* **1980**, *73*, 3688.
(31) Weber, T. A. *J. Chem. Phys.* **1978**, *69*, 2347.
(32) Weber, T. A. *J. Chem. Phys.* **1978**, *70*, 4277.
(33) Evans, G. T.; Knauss, D. C. *J. Chem. Phys.* **1980**, *72*, 1509.
(34) Knauss, D. C.; Evans, G. T. *J. Chem. Phys.* **1980**, *72*, 1499.
(35) Knauss, D. C.; Evans, G. T. *J. Chem. Phys.* **1980**, *73*, 3423.
(36) Pear, M. R.; Weiner, J. H. *J. Chem. Phys.* **1979**, *71*, 212.
(37) Pear, M. R.; Weiner, J. H. *J. Chem. Phys.* **1980**, *72*, 3939.
(38) McCammon, J. A.; Northrup, S. H.; Karplus, M.; Levy, R. M. *Biopolymers* **1980**, *19*, 2033.
(39) Pear, M. R.; Northrup, S. H.; McCammon, J. A.; Karplus, M.; Levy, R. M. *Biopolymers* **1981**, *20*, 629.
(40) Evans, G. T. *J. Chem. Phys.* **1980**, *72*, 3849.
(41) Ladanyi, B. M.; Hynes, J. T. *J. Chem. Phys.* **1982**, *77*, 4739.
(42) Tropp, J. *J. Chem. Phys.* **1980**, *72*, 6035.
(43) Fixman, M.; Kovac, J. *J. Chem. Phys.* **1974**, *61*, 4939.
(44) Fixman, M.; Kovac, J. *J. Chem. Phys.* **1974**, *61*, 4950.
(45) Vacatello, M.; Avitabile, G.; Corradini, P.; Tuzi, A. *J. Chem. Phys.* **1980**, *73*, 548.
(46) Warchol, M. P.; Vaughan, W. E. *J. Chem. Phys.* **1977**, *67*, 486.
(47) Evans, G. T. *Mol. Phys.* **1978**, *36*, 1199.
(48) Evans, G. T. *J. Chem. Phys.* **1978**, *69*, 3363.
(49) Evans, G. T. In "Molecular-Based Study of Fluids" (Advances in Chemistry Series, No. 204); American Chemical Society: Washington, D.C., 1983; Chapter 17.
(50) Crossley, J. *J. Adv. Mol. Relaxation Processes* **1974**, *6*, 39.
(51) Champion, J. V.; Dandridge, A.; Meeten, G. H. *Faraday Discuss. Chem. Soc.* **1979**, *66*, 266.
(52) Kivelson, D.; Madden, P. A. *Annu. Rev. Phys. Chem.* **1980**, *31*, 523.
(53) Doddrell, D.; Allerhand, A. *J. Am. Chem. Soc.* **1971**, *93*, 1558.
(54) Lyerla, J. R., Jr.; McIntyre, H. M.; Torchia, D. A. *Macromolecules* **1974**, *7*, 11.
(55) Lyerla, J. R., Jr.; Horikawa, T. T. *J. Phys. Chem.* **1976**, *80*, 1106.
(56) Redfield, A. G. *IBM J. Res. Develop.* **1957**, *1*, 19.
(57) Redfield, A. G. *Adv. Mag. Reson.* **1965**, *1*, 1.

Scheme I

i. $C_4D_9{}^{13}CH_2C_4D_9$ (IV):

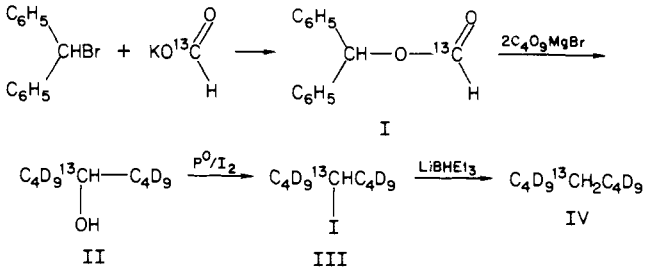

ii. $C_{10}D_{21}{}^{13}CH_2C_{10}D_{21}$ (VIII):

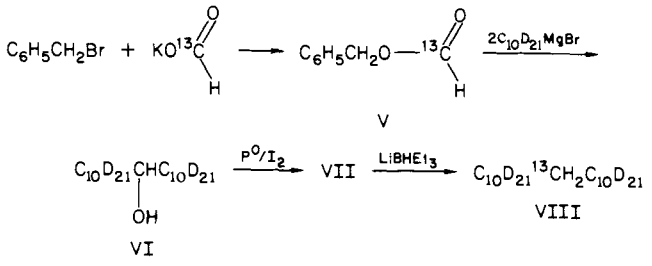

iii. $C_7D_{15}{}^{13}CH_2CD_3$ (XIII)

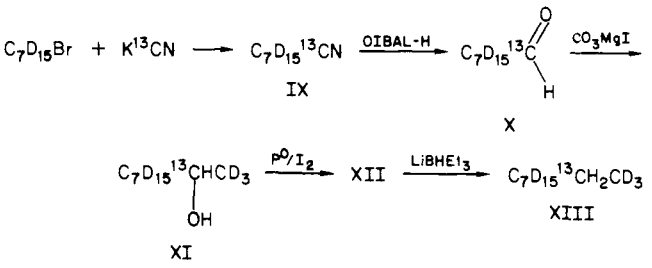

the middle of the chain could be observed. The final methylene group at the chain extremity is C-2. The C-2 methylene is a more reliable probe of the rotational dynamics than the C-1 carbon because the very rapid rotation of methyl groups obscures the chain's dynamics. Nonane was finally selected since it satisfied the above criteria; in addition, nonane is a relatively nonvolatile liquid that dissolves easily in a variety of solvents over a wide range of temperatures. Heneicosane was chosen because its chain is longer than nonane by more than a factor of 2. Also, the nontrivial synthesis of these labeled compounds placed some limits on the molecules to be studied. Geometrical parameters (bond lengths, bond angles) have been determined previously using X-ray diffraction of crystalline *n*-alkanes,[58,59] electron diffraction of gaseous *n*-alkanes from propane to heptane,[60] and the microwave spectrum of propane.[61]

II. Experimental Section

A. Synthesis of Labeled Alkanes. Coupled relaxation studies on the AX_2 spin system necessitated labeled compounds with the following specifications: (1) the compound must be enriched in ^{13}C at only one, nonmethyl position; (2) the ^{13}C must bear two protons; and (3) all other hydrogen in the molecule must be deuterium to approximate the AX_2 conditions. These three requirements place considerable restrictions on the synthetic strategies. First, the choice of starting materials is limited to those readily available from companies selling labeled materials. Second, the synthetic scheme must avoid reactions which scramble and/or exchange protons. Third, any separations involved should also maintain the integrity of the isotopic labeling.

The synthetic schemes for each of the three compounds made for this work are given in Scheme I. Specific synthetic details are given in Appendix I.

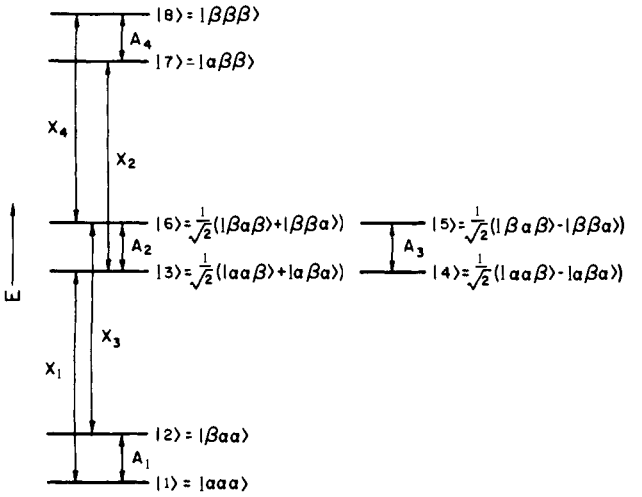

Figure 1. Energy level diagram for an $AX_2(^{13}CH_2)$ spin system defining the eigenstates and the allowed transitions.

B. Shear Viscosity Measurements. The Brownian dynamics simulations require values for the shear viscosity to obtain absolute values for the rotational correlation times. To avoid opening the sealed NMR samples, the viscosity of ordinary unlabeled deglyme was determined. Ordinary techniques utilizing an Ostwald viscometer and a pycnometer, such as described by Shoemaker,[62] were used to measure the shear viscosity of near diglyme at 273, 313, and 353 K. The temperatures for these experiments are considered accurate to ±0.25 K. Three runs at each temperture were made for each measurement of flow times for both the neat diglyme and reference water. The reference water had a resistance of 17.5 MΩ. The values used for the viscosity of water at the various temperature[63] were not corrected for pressure. The values obtained for the shear viscosity, η, are 0.69 cP at 353 K, 1.04 cP at 313 K, and 2.39 cP at 273 K. The value for the viscosity of diglyme at 233 K was determined to be 5.9 cP by plotting ln η vs. $1/T$ and extrapolating to 233 K.

C. Choice of Solvents. Many of the theoretical and computer studies of alkane chains have been performed assuming a neat sample of the hydrocarbon. In order for the NMR relaxation results to be comparable with such analyses, perdeuteriodiglyme was used as the solvent for the nonane systems. Perdeuteriodiglyme, $(CD_3OCD_2CD_2)_2O$, is a nine-segment chain that is isoelectronic to nonane with few more degrees of rotational freedom at the ether linkages. Also, many of the physical properties of diglyme (such as boiling point, melting point, and density) are similar to those of nonane. Thus, the spin-labeled nonanes dissolved in perdeuteriodiglyme form a system that closely emulates neat nonane. The use of a deuterated solvent increases the magnetic isolation of the $^{13}CH_2$ spin system and also provides a deuterium lock signal. As the synthesis of the labeled 5-nonane was completed before the arrival of the perdeuteriodiglyme, a sample of the 5-nonane dissolved in CD_2Cl_2 was prepared for preliminary experiments. While temperature studies were not done on this sample, the results from this sample provided some insight into the effect of solvent on chain motion.

D. NMR Experiments. The relaxation experiments were performed on a modified Varian XL-100-15 spectrometer equipped with a 16K Varian 620L-100 computer and a homemade pulsed spin decoupler based on a Hewlett-Packard Model 5105A frequency synthesizer. This system, and the method of data collection, has been previously described.[7] The system has since been modified so that the spectrometer's 620L computer is interfaced via a serial communications link to a PDP 11/34 computer, equipped with a Computer Labs/pertec disk system. The communications network utilizes hardware and software drivers previously described.[64] Data are acquired in the following fashion: first, all the different parameter sets are created on the 620L computer and stored

(58) Bowen, H. J. M.; Sutton, L. E. "Tables of Interatomic Distances and Configurations in Molecules and Ions"; The Chemical Society: London, 1958.
(59) Shearer, H. M. M.; Vand, V. *Acta Crystallogr.* **1956**, *9*, 379.
(60) Bonham, R. A.; Bartell, L. S.; Kohl, D. A. *J. Am. Chem. Soc.* **1959**, *81*, 4765.
(61) Lide, D. R. *J. Chem. Phys.* **1960**, *33*, 1514.
(62) Shoemaker, D. P.; Garland, C. W.; Steinfeld, J. I. "Experiments in Physical Chemistry"; McGraw-Hill: New York, 1974.
(63) Weast, R. C., Ed. "Handbook of Chemistry and Physics"; The Chemical Rubber Co.: Cleveland, Ohio, 1971; Vol. 52.
(64) Alderman, D. W.; Hamill, W. D., Jr.; Mayne, C. L.; Grant, D. M. In "The University of Utah NMR Laboratory Minicomputer Network" (Computer Networks in the Analytical Chemistry Laboratory); Wiley-Interscience: New York, 1981.

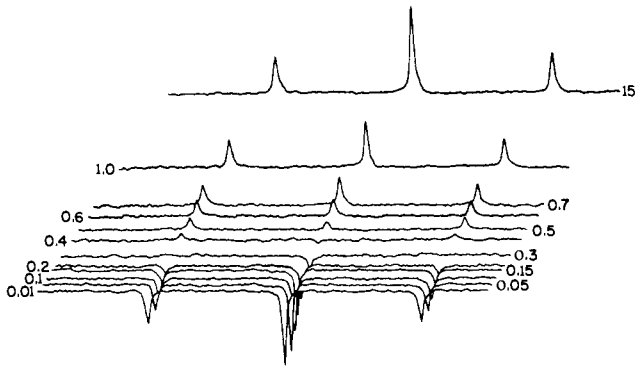

Figure 2. ^{13}C spectra from a coupled inversion recovery experiment on $C_4D_9{}^{13}CH_2C_4D_9$ dissolved in perdeuteriodiglyme at 233 K, showing the time evolution of the carbon triplet after a hard carbon π pulse.

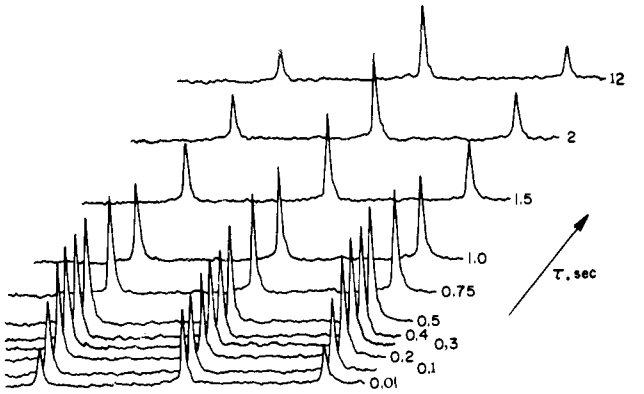

Figure 3. ^{13}C spectra from a hard pulse experiment on $C_4D_9{}^{13}CH_2C_4D_9$ dissolved in perdeuteriodiglyme at 233 K, showing the time evolution of the carbon triplet after a hard proton π pulse.

on the PDP 11/34 disk. The 620L computer then solicits a parameter file from the PDP 11/34 and collects one transient using those parameters, after which it returns the parameters and FID to the PDP 11/34 for storage on this disk. This process is repeated for each parameter set having a different τ value (the time between the perturbing and observe pulses). For shorter recycle delays, a version of the program was developed which takes several transients on a file before transferring the FID to the PDP 11/34. The sequence of τ values was scrambled, so that data points at the same section of the relaxation curve are collected at different times in the cycle. As previously discussed,[7] these procedures average out spectrometer drift and variations in sensitivity over all data points. This was particularly important in the longer (up to several days) runs in this study.

Relevant spectrometer parameters for the alkanes are: spectral width, 1024 Hz; acquisition time, 4 s; exponential time constant, 0.2 s; recycle delays ranging from 10 s for nonane at 233 K to 150 s for nonane at 353 K, adjusted to be at least 10 times the nominal T_1 of the sample. The alkane coupling constants are all 124 Hz.

Three different preparations of the spin systems were used. In the coupled inversion recovery (CIR) experiment, a carbon 180° pulse inverts the three carbon lines. This exchanges energy levels 1 and 2, 3 and 5, 4 and 6, and 7 and 8 (see Figure 1). In the hard pulse (HP) experiment a high power 180° pulse at the proton chemical shift frequency is used to invert both proton lines, thereby exchanging levels 1 and 7 and 2 and 8. In the soft pulse (SP) experiment a low power 180° pulse is applied to only one line of the proton doublet. This exchanges either levels 1 and 7 or 2 and 8. Following the spin system preparation, the system is allowed to evolve for a time τ, followed by a 90° observe pulse in the carbon-13 domain. The resulting free induction decays are collected and Fourier transformed, and the partially relaxed line intensities measured.[8] It is important to note that the decoupler remains off throughout the experiment. The hard pulse experiments were performed using 10 w of decoupler power irradiating a single frequency midway between the two proton lines, with a proton 180° pulse width of 180 μs.

The amplitude, frequency, and duration of the soft proton pulse were optimized by comparing the carbon magnetization with τ set to zero with that of a coupled spectrum and obtaining as nearly as possible the correct initial carbon relative intensities of −6.95:2.0:8.95. Because of the deuterium broadened proton line widths, it was found that a simple low power proton pulse did not provide sufficient perturbation. Also, in the case of the chain molecules, the relaxation times involved are fast enough that significant relaxation occurs during the very low power pulses (which are on the order of 150 ms). For these reasons an intermediate soft pulse as described by Bovee[13] was used. The proton rf field is set so that the 180° pulse time τ equals $3^{1/2}/(2J_{CH})$; thus, when a 180° pulse is applied on resonance to one line, the other line of the doublet nutates through 360° about its effective field in the rotating frame and is effectively unperturbed. The amplitude of the pulse was controlled within ±10% for a pulse width of 7.0 ms.

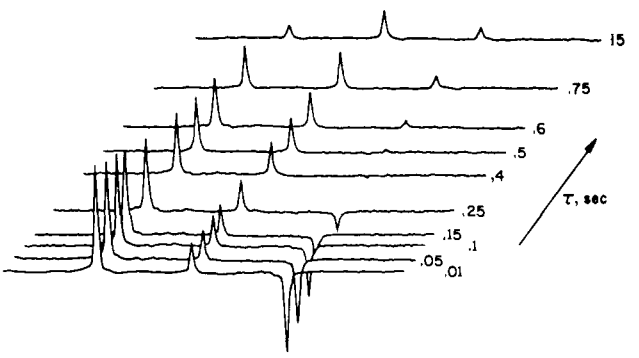

Figure 4. ^{13}C spectra from a medium-soft pulse experiment in which one porton line is inverted 180° and the other proton line rotated through 360°.

For each of the different experiments, 23 to 31 different data points were collected. A few points in each run, usually eight, were duplicated with the same τ value, to ensure reproducibility. All three experiments were performed at 233, 273, 313, and 353 K on the nonane samples, and 313, 353, and 393 K on the heneicosane sample (which freezes at slightly above room temperature). Temperatures are estimated to be accurate to about ±1 K.

III. Relaxation Data and Results

A typical set of the relaxation data is shown in Figure 2–4 for the 5-nonane in perdeuteriodiglyme at −40 °C. Several interesting features distinguish the data from that obtained in earlier studies. The coupled inversion recovery experiment (Figure 2) shows very clearly that the two outer lines of the carbon triplet relax more quickly than the central line. The extent of this difference in recovery rates relates directly to the contribution of the J_{HCH} power density and can be seen most clearly around the point where the magnetization passes through zero. The alkane data exhibit this effect more clearly than any of the data taken on the methylene halides[7,8] or on cyclopropane.[15] Figure 3 contains the data from a hard pulse experiment. The outer lines increase in intensity as τ increases, until they pass through a maximum and begin to decrease. The departure of the relative intensities from the 1:2:1 triplet shows primarily the contribution of J_{CHH} to the relaxation. As can be seen from Figure 3, the effect is quite pronounced in the case of the alkanes. The data from the intermediate soft pulse experiment are given in Figure 4. The slight rise in the center line, which is small compared with the dramatic changes in the other lines, is due to imperfections in the spectrometer intermediate soft pulse. Thus, a slight amount of hard pulse character is observed.

A. Fits of the Data. All of the alkane data were fit using both the magnetization mode fit (MMF) and line intensity fit (LIF) routines as described previously;[8] the results from the two routines were found to be within one standard deviation of each other for each set of data. In this analysis it was more convenient to use the MMF fit, and these results are given in Table I. The parameters for the fits in Table I are the four dipolar spectral densities J_{CH}, J_{HH}, J_{HCH}, and J_{CHH}, the carbon autocorrelation random field spectral density j_C (locked to zero), and the proton auto- and cross-correlation random field terms j_H and j_{HH} (locked together). Other spectrometer parameters used in the fits but not reported in Table I are four pulse efficiency factors α; three scaling parameters, K; and five other factors, ω. The four pulse efficiency parameters α express the efficiency of the 180° pulse in inverting level populations. In the ideal case α equals unity, but the ex-

Table I. Values of the Fitted Parameters for 5-Nonane Dissolved in Perdeuteriodiglyme and CD_2Cl_2, 2-Nonane in Perdeuteriodiglyme, and 11-Heneicosane in Perdeuteriodiglyme

5-Nonane ($C_4D_9{}^{13}CH_2C_4D_9$) Dissolved in Perdeuteriodiglyme $(CD_3OCD_2CD_2)_2O$ and CD_2Cl_2

	233 K	233 K	273 K	313 K	353 K
J_{CH}	0.078 ± 0.001	0.291 ± 0.005	0.063 ± 0.001	0.026 ± 0.003	0.015 ± 0.001
J_{HH}	0.084 ± 0.005	0.310 ± 0.030	0.065 ± 0.003	0.028 ± 0.001	0.018 ± 0.001
J_{HCH}	0.018 ± 0.002	0.100 ± 0.010	0.022 ± 0.001	0.009 ± 0.001	0.004 ± 0.001
J_{CHH}	0.057 ± 0.002	0.235 ± 0.009	0.047 ± 0.001	0.019 ± 0.001	0.011 ± 0.001
j_C	0	0	0	0	0
$j_H = j_{HH}$	0.006 ± 0.003	0.072 ± 0.020	0.005 ± 0.002	0.002 ± 0.001	0.001 ± 0.001

2-Nonane ($C_7D_{15}{}^{13}CH_2CD_3$) Dissolved in $(CD_3OCD_2CD_2)_2O$

	233 K	273 K	313 K	353 K
J_{CH}	0.206 ± 0.003	0.049 ± 0.001	0.0204 ± 0.0003	0.0114 ± 0.0002
J_{HH}	0.193 ± 0.013	0.045 ± 0.003	0.0152 ± 0.0011	0.0106 ± 0.0006
J_{HCH}	0.061 ± 0.006	0.007 ± 0.002	0.0037 ± 0.0006	0.0015 ± 0.0004
J_{CHH}	0.146 ± 0.004	0.034 ± 0.001	0.0136 ± 0.0004	0.0071 ± 0.0002
j_C	0	0	0	0
$j_H = j_{HH}$	0.057 ± 0.009	0.019 ± 0.003	0.0074 ± 0.0009	0.0022 ± 0.0004

11-Heneicosane ($C_{10}D_{21}{}^{13}CH_2C_{10}D_{21}$) Dissolved in $(CD_3OCD_2CD_2)_2O$

	313 K	353 K	393 K
J_{CH}	0.110 ± 0.001	0.055 ± 0.001	0.038 ± 0.001
J_{HH}	0.098 ± 0.005	0.060 ± 0.002	0.037 ± 0.002
J_{HCH}	0.040 ± 0.002	0.020 ± 0.001	0.012 ± 0.001
J_{CHH}	0.082 ± 0.002	0.040 ± 0.001	0.027 ± 0.001
j_C	0	0	0
$j_H = j_{HH}$	0.015 ± 0.003	0.003 ± 0.001	0.002 ± 0.001

perimental values of α range from about 0.85 to 0.99. The five ω parameters compensate for the fact that the ratio of the line intensities of the carbon-13 triple deviate slightly from the expected 1:2:1 ratio because of spectrometer imperfections such as pass-band ripple of the filters used in processing the transient before it is digitized. The ω's are always quite small in a successful experiment (less than 0.1) but are necessary to account for small systematic errors in the experiment. These parameters are available upon request.

All fits reported here have the j_C carbon random field term locked to zero, since zero is always within one standard deviation if this parameter is allowed to vary in the fit. The proton randon field terms, j_H and j_{HH}, are also locked together since they too are statistically indistiguishable when allowed to vary separately. The coordinate system was described in the previous paper,[1] with the y axis directed parallel to the H–H vector, the x axis bisecting the HCH bond angle, and the z axis perpendicular to the HCH plane.

Typical fits of the data are shown in Figures 5–7 for 2-nonane in diglyme at 353 K.

B. Results. The values of the fitted parameters, along with the estimates of their marginal standard deviations, are given in Table I. The quantities of greatest relevance from these fits are the four dipolar power densities J_{CH}, J_{HCH}, J_{CHH}, and J_{HH}, which are transformed into the Cartesian correlation times as described in the previous paper.[1] The error estimates in the Cartesian correlation times are obtained by transforming the covariance matrix for the fit and calculating the marginal standard deviation in the reduced Cartesian basis. A bond angle of 108.5° and a carbon–proton bond length of 1.12 Å were used in the transformation to Cartesian power densities and correlation times. These structural parameters were obtained from the corresponding average values taken from electron diffraction data on gaseous n-alkanes from propane to heptane.[60]

IV. Interpretation and Analysis

A. Theoretical Model for Chain Dynamics. Brownian dynamics (BD) modeling provides a relatively simple yet reasonable representation of the dynamics of a flexible chain molecule in a liquid. In one variation of the model, due to Fixman,[24,25] the chain molecule has rigidly constrained bond lengths and nearest-neighbor bond angles. Differential potentials control the relative positions and motion of the nonbonded atoms. As a result of the frequent collisions of the chain molecule with the solvent, the chain is assumed to obey a diffusion equation subject to the intramolecular forces discussed above. In the BD algorithm each backbone atom (here a methylene carbon) moves because of the Gaussian random forces exerted during collisions with the solvent but is constrained by the intramolecular forces, which guarantee the correct shape of the chain. The length of a positional displacement is inversely proportional to the translational friction coefficient per backbone atom, f. Since the potential parameters and shape of the alkanes are known, f is the only adjustable parameter in the calculation, and all the correlation times scale linearly with this parameter.

In this work, the four Cartesian correlation times τ_{xx}, τ_{yy}, τ_{zz}, and τ_{xy} derived[1] for an AX_2 spin system are calculated for nonane using BD. In Figure 8, a bond vector coordinate system is defined, in which each of the eight bond vectors, ($\tilde{b}_i$, i = 1–8), of nonane lies along a specific C–C bond. A Cartesian coordinate system on carbon i is defined using the bond vectors. In this system, the z axis points generally along the local chain contour as it is perpendicular to the HCH plane. Thus,

$$\hat{e}_z(i) = (\tilde{b}_i + \tilde{b}_{i+1})/|\tilde{b}_i + \tilde{b}_{i+1}| \quad (1)$$

and the x axis bisects the HCH angle

$$\hat{e}_x(i) = (\tilde{b}_i - \tilde{b}_{i+1})/|\tilde{b}_i - \tilde{b}_{i+1}| \quad (2)$$

and the y axis is orthogonal to $\hat{e}_x(i)$ and $\hat{e}_z(i)$, as shown in Figure 8.

$$\hat{e}_y = \hat{e}_z \times \hat{e}_x \quad (3)$$

The simulations calculate and the experiments measure the correlation times associated with the second-rank tensors constructed from the $\hat{e}_x$, $\hat{e}_y$, and $\hat{e}_z$ unit vectors.

The Brownian dynamics simulations were performed on a nonane-like molecule with rigidly constrained bond lengths and nearest-neighbor bond angles held at 110°. Torsional fluctuations were controlled by the Ryckaert-Bellemans potential,[23] and the pentane and excluded volume effects were incorporated by including the Lennard-Jones (LJ) 6–12 interaction between nonbonded atoms in the chain. LJ parameters were also taken from Ryckaert and Bellemans.[23]

Correlation times τ_{xx}, τ_{yy}, τ_{zz}, and τ_{xy} were calculated during 100 trajectories of the BD simulation. Each trajectory used a time step of 0.001 reduced time units and had a duration of 9.6 units of time. The unit of time is fb^2/k_BT, where b is the C–C bond

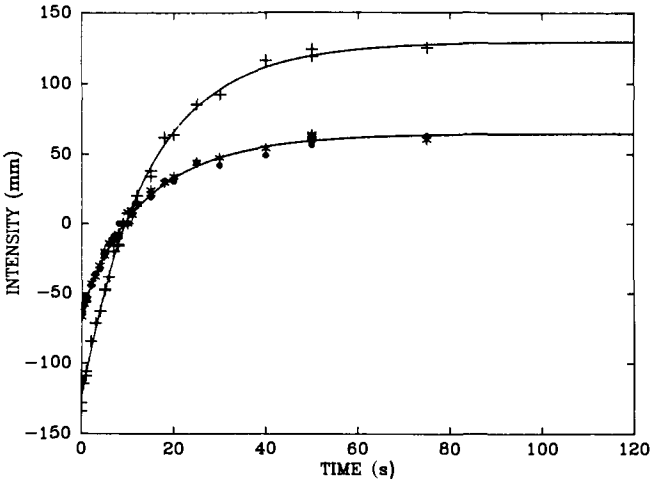

Figure 5. Plot of the results of a nonlinear least-squares fit of the data for the coupled inversion recovery experiment on $C_7D_{15}{}^{13}CH_2CD_3$ dissolved in perdeuteriodiglyme at 353 K.

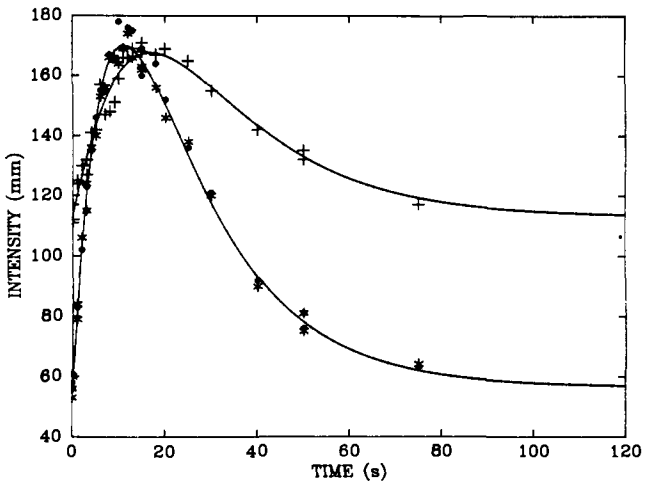

Figure 6. Plot of the results of a nonlinear least-squares fit of the data for the proton hard pulse experiment on $C_7D_{15}{}^{13}CH_2CD_3$ dissolved in perdeuteriodiglyme at 353 K.

length, k_B the Boltzmann constant, and T the temperature. Each of the correlation times was determined by fitting the short time decay of the correlation functions to a power law decay and the long time behavior to an exponential function and integrating each contribution analytically. Uncertainties in the computed times range from 10 to 20%. To derive absolute values of the calculated correlation times for nonane, one must specify a model for the translational friction coefficient of a backbone atom. Previously[49] it was found that f could be approximated by a Stokes law model with stick boundary conditions (relating to the fluid surrounding the backbone atom) and so

$$f = 6\pi\eta(b/2) \tag{4}$$

where η is the zero frequency shear viscosity and $b/2$ is the hydrodynamic radius of the backbone atom.

B. Comparison of Experimental and Calculated Correlation Times. Table II gives the values of the Cartesian correlation times τ_{xx}, τ_{yy}, τ_{zz}, and τ_{xy} obtained by transformation of the fitted dipolar spectral densities, along with the same correlation times as predicted by the Brownian dynamics simulations. For convenience in the discussion, the table lists the anisotropy ratios τ_{zz}/τ_{xy} and τ_{yy}/τ_{xy}. Other quantities in Table II include the ratios of the various correlation times at different segments of the chain (e.g., τ_{xx}(C-5)/τ_{xx}(C-2)).

Comparison of the correlation times obtained from the NMR measurements and the BD simulations show good agreement, and the general qualitative trends are well reproduced. First, both

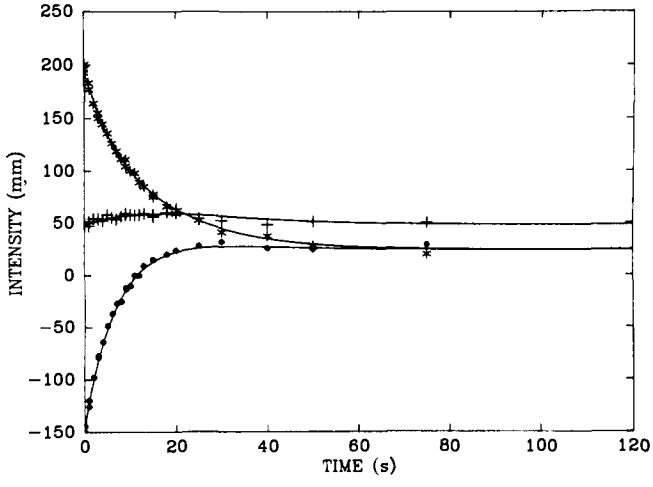

Figure 7. Plot of the results of a nonlinear least-squares fit of the data for the medium-soft pulse experiment on $C_7D_{15}{}^{13}CH_2CD_3$ dissolved in perdeuteriodiglyme at 353 K.

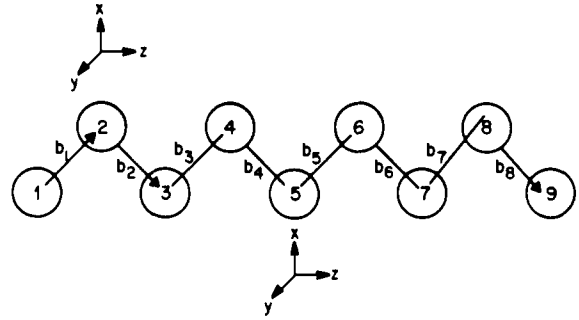

Figure 8. Coordinate system for the Brownian dynamics simulation of nonane.

the dynamics calculations and the experimental values agree that the rotational motion at both the middle and terminal methylene segments has local prolate symmetric-top character:

$$\tau_{zz} > \tau_{xx},\ \tau_{yy} > \tau_{xy} \tag{5}$$

in accord with eq 27 of paper 1. Actually, the τ_{xx} are rather poorly determined experimentally compared with the other correlation times and highly correlated to the τ_{yy}. Thus the experimental verification of the symmetric-top character is limited. The gradient of the correlation time obeys an inequality:

$$\frac{\tau_{zz}(\text{C-5})}{\tau_{zz}(\text{C-2})} > \frac{\tau_{xx}(\text{C-5})}{\tau_{xx}(\text{C-2})},\ \frac{\tau_{yy}(\text{C-5})}{\tau_{yy}(\text{C-2})} > \frac{\tau_{xy}(\text{C-5})}{\tau_{xy}(\text{C-2})} \tag{6}$$

which is consistent with the interpretation that the dephasing of τ_{zz} for carbon 5 requires a considerable amount of solvent displacement; hence this mode is slower than the dephasing rate at carbon 2. At the other extreme, the xy functions dephase at nearly the same rate independent of chain position at each temperature (except 233 K), and in each case the τ_{xy} values are always much smaller than the other three correlation times. This result is quite reasonable since the xy spatial function is dephased by all angular displacements, and even the small torsional fluctuations about the long axis at the chain center are apparently sufficient to cause the relaxation of the xy function. BD simulations[65] and NMR measurements[54] of the T_1 of heptane have also indicated the presence of small gradients in the relaxation times. However, the combination of small chain length and NMR measurements of T_1, which measures a mixture of modes, prohibited a clear distinction between the chain-length-dependent and chain-length-independent properties in these previous investigations.

(65) Levy, R. M.; Karplus, M. In ref 49, Chapter 18. See also: Levy, R. M.; Karplus, M.; Wolynes, P. G. *J. Am. Chem. Soc.* **1981**, *103*, 5998.

Table II. Cartesian Correlation Times (in picoseconds) Obtained from the NMR Relaxation Experiments and Calculated with Brownian Dynamics (BD) Simulations[a]

	5-nonane in $(CD_3OCD_2CD_2)_2O$		2-nonane in $(CD_3OCD_2CD_2)_2O$		ratio τ_{ij}(C-5)/τ_{ij}(C-2)	
	exptl	BD	exptl	BD	exptl	BD
			T = 353 K, η = 0.69 cP			
τ_{xx}	5.5 ± 1.4	4.0	2.6 ± 0.8	3.0		
τ_{yy}	3.9 ± 0.2	4.2	2.2 ± 0.1	2.9	1.7	1.4
τ_{zz}	6.6 ± 0.5	11.0	4.4 ± 0.4	5.8	1.5	1.8
τ_{xy}	1.4 ± 0.1	2.5	1.3 ± 0.1	2.1	1.1	1.2
τ_{zz}:τ_{yy}:τ_{xy}	(4.6:2.7:1)	(4.2:1.6:1)	(3.2:1.7:1)	(2.8:1.4:1)		
			T = 313 K, η = 1.04 cP			
τ_{xx}	7.0 ± 2.0	8.5	0.7 ± 2.0	6.1		
τ_{yy}	5.9 ± 0.3	9.4	3.2 ± 0.2	5.9	1.8	1.6
τ_{zz}	12.5 ± 0.8	25.0	7.1 ± 0.7	12.0	1.8	2.1
τ_{xy}	2.3 ± 0.1	5.0	2.3 ± 0.1	4.4	1.0	1.1
τ_{zz}:τ_{yy}:τ_{xy}	(5.6:2.6:1)	(5:1.9:1)	(3.1:1.4:1)	(2.7:1.4:1)		
			T = 273 K, η = 2.39 cP			
τ_{xx}	12 ± 4.0	23	4 ± 4.0	17		
τ_{yy}	14 ± 0.6	23	9 ± 0.7	18	1.4	1.3
τ_{zz}	28 ± 2.0	64	16 ± 2.0	36	1.7	1.8
τ_{xy}	6 ± 0.2	13	6 ± 0.2	12	1.0	1.1
τ_{zz}:τ_{yy}:τ_{xy}	(4.9:2.4:1)	(4.9:1.8:1)	(2.9:1.7:1)	(3:1.5:1)		

	5-nonane in CD_2Cl_2 exptl	5-nonane in $(CD_3OCD_2CD_2)_2O$		2-nonane in $(CD_3OCD_2CD_2)_2O$		ratio τ_{ij}(C-5)/τ_{ij}(C-2)	
		exptl	BD	exptl	BD	exptl	BD
			T = 233 K, η = 5.9 cP (extrapolated value)				
τ_{xx}	14 ± 6.0	29 ± 36	64	39 ± 17	58		
τ_{yy}	18 ± 1.0	65 ± 6	71	41 ± 3	57	1.6	1.3
τ_{zz}	29 ± 3.0	113 ± 14	193	90 ± 8	123	1.3	1.6
τ_{xy}	8 ± 0.3	26 ± 1	42	20 ± 1	41	1.3	1.0
τ_{zz}:τ_{yy}:τ_{xy}	(3.5:2.2:1)	(4.3:2.5:1)	(4.6:1.7:1)	(4.5:2.1:1)	(3:1.4:1)		

	Heneicosane in $(CD_3OCD_2CH_2)O$		
	313 K	353 K	393 K
τ_{xx}	13 ± 6.0	17 ± 2.0	8 ± 2.0
τ_{yy}	21 ± 1.0	13 ± 0.4	8 ± 0.3
τ_{zz}	48 ± 3.0	27 ± 1.0	17 ± 0.8
τ_{xy}	9 ± 0.3	5 ± 0.1	4 ± 0.1
τ_{zz}:τ_{yy}:τ_{xy}	(5.1:2.2:1)	(5.6:2.7:1)	(4.8:2.3:1)

[a] The experimental viscosities of diglyme were measured at 353, 313, and 273 K, and extrapolated to 233 K. Errors are given as one marginal standard deviation.

The experimental and theoretical anisotropy ratios are in good agreement at all temperatures except 233 K. For example, for the 5 position of nonane at 273 K the NMR results show the ratios τ_{zz}:τ_{yy}:τ_{xy} to be 4.9:2.4:1 with the BD predictions giving 4.9:1.8:1. For the 2 positions at 273 K, the experimental anisotropies are 2.9:1.7:1 compared with the theoretical values 3:1.5:1. The agreement in the dimensionless quantities such as the gradients and anisotropy ratios is interpreted as an indication that the torsional and LJ potential used in the BD algorithm represent the basic energetics at the two locations in the nonane chain. The ratio of τ_{yy} to τ_{xy} at the 5 position is slightly underestimated by the dynamics simulation over the entire temperature range.

The absolute values of the calculated times are closest to the experimental values at the highest temperatures, where the experimental times are smaller than the theoretical times by about 25%. It should be noted that the 25% agreement at the highest temperature lends credibility to the model used for the friction coefficient. As temperature decreases, the deviations increase, and at the lowest temperatures (233 K) the calculated times are greater than the experimental values by a factor of roughly 2. Also, at 233 K, the observed anisotropy ratios and gradients differ by the greatest amount from the calculated values. The experiments indicate that the anisotropy at carbon 2 is nearly the same as the anisotropy at carbon 5, whereas BD predicts a smaller anisotropy at the terminal methylene, as is the case at the higher temperatures. The xy gradient at 233 K shows significant deviation from the BD predictions and from its behavior at higher temperature, where it was always nearly unity.

Several approximations in the BD model could be responsible for discrepancies in the temperature dependence of the theoretical and experimental correlation times: (1) inertial effects, (2) potential energy functions, (3) hydrodynamic interactions (HI), (4) frequency dependence of the shear viscosity, and (5) nonspherical solvent alignment. These five factors will be considered in the following paragraphs.

The BD algorithm used in the simulations ignored the mass of the isomerizing backbone atoms, and, as a consequence, inertial effects are absent from the model. Processes such as streaming over barriers (i.e., free convection) always increase the correlation times relative to the BD estimates.[66-68] Since the BD times are larger than the experimental values, inclusion of inertial corrections can only cause the observed deviation to increase.

The potential energy functions employed in the BD simulations incorporated a trans–gauche energy difference, E_{TG}, of 700 cal/mol, whereas recent Raman measurements[69] indicate that E_{TG} is closer to 550 cal/mol. It seems unlikely that the 150-cal/mol differences in energies could be responsible for the discrepancies for two reasons. First, the energy difference is relatively small, and, second, the gradients in the correlation times and their anisotropies are in good agreement at the high temperatures, in-

(66) Skinner, J. L.; Wolynes, P. G.; *J. Chem. Phys.* **1978**, *69*, 2143.
(67) Northrup, S. H.; Hynes, J. T. *J. Chem. Phys.* **1980**, *73*, 2700.
(68) Evans, G. T. *J. Chem. Phys.* **1983**, *78*, 4963.
(69) Wong, P. T. T.; Mantsch, H. H.; Snyder, R. G. *J. Chem. Phys.* **1983**, *79*, 2369.

dicating that the potential functions in the alkane are reasonable.

The neglect of hydrodynamic interactions[70] could also be a reason for disagreement of theory and experiment. The HI tensor contributions to the atomic diffusion coefficients varies as $(\eta \cdot r_{ij}(t))^{-1}$, where r_{ij} is the distance between backbone atoms i and j. This is contrasted with the ordinary diffusion coefficient which varies as ηb. However, for small stiff chains like nonane, the difference in the extremes of the fluctuations in $r_{ij}(t)$ as a function of temperature will probably be too small to account for the observed discrepancy (i.e., less than the necessary factor of 2). The implementation of HI should decrease the calculated correlation times, but by a nearly temperature-independent constant.

A fourth possible cause for the discrepancy in the temperature dependence can be traced to the frequency dependence of the shear viscosity. Hynes[71,72] has suggested that in high viscosity liquids, isomerizing molecules do not experience the full zero frequency shear viscosity, $\eta(0)$, but instead sample the viscosity, $\eta(\omega_b)$, evaluated at a frequency, ω_b, determined by the curvature of the barrier separating the isomers. In low viscosity liquids, $\eta(0) = \eta(\omega_b)$; however, with increasing viscosity, $\eta(\omega_b)$ falls below $\eta(0)$. As a result, the effective friction on the isomerizing molecule does not track the zero frequency shear viscosity. Recent picosecond optical experiments[73,74] have provided support for this hypothesis. The Hynes explanation would account for BD results overestimating the correlation times and the degradation of the agreement at the higher viscosities. The difficulty in applying the Hynes model directly to the present problem is that the NMR correlation times have contributions from overall as well as internal rotation, and a significant body of data supports the notion that overall rotation is determined by the zero frequency viscosity.[49] Nonetheless, the frequency-dependent shear viscosity would provide a sensible and at least qualitative explanation of the temperature dependence of the correlation times.

Finally, the fifth weakness in the BD simulations arises from the improper handling of the nonspherical nature of the solvent. As discussed in the previous paragraph, the temperature dependence of the correlation times over the interval 273–353 K could be explained qualitatively using the Hynes friction argument. The experimental results at 233 K, however, indicate that the local anisotropies at carbon 2 and 5 are nearly the same, contrary to the theoretical prediction of less anisotropy at the terminal methylene. The BD algorithm already incorporates torsional potentials that favor the all-trans conformation at low temperatures, but the experiments at 233 K indicate that the chain has more rod-like character than would be expected on the basis of the single particle torsional potential. This enhanced trans preferrence could be attributable to the solvent, perdeuteriodiglyme, which also adopts a trans configuration at low temperatures like the solute molecules. Thus, the solvent–solute system might be showing evidence of the formation of an ordered (all-trans) phase. This conjecture is supported by the experimental results at 233 K for 5-nonane dissolved in CD_2Cl_2 (a more spherical solvent) since the anisotropy is smaller in methylene chloride than in diglyme. The experimental correlation times in methylene chloride are roughly one-third the corresponding times in diglyme, as would be expected in a less viscous solvent.

Experimental correlation times for the central carbon (C-11) in heneicosane were also determined. Heneicosane moves more slowly than nonane at the same temperature, with the correlation times 3.3 to 4.4 times longer than those for the central carbon in nonane (C-5). The anisotropy ratios in the C_9 and C_{21} chains are within experimental error of each other. BD simulations were not conducted on the C_{21} system, primarily because of cost and time restrictions. A typical BD run on heneicosane would last 10 times longer than a nonane simulation. Even in the absence of firm simulation data, some interpretations of the results can still be made for heneicosane for comparison with the results on nonane.

Although there are no simple analytical expressions for realistic models of chain molecules applicable to the correlation times discussed in this study, the Rouse–Zimm, or bead-spring model,[70] can at least estimate the lowest frequency mode of the chain. BD studies of medium-sized alkanes have confirmed that the lowest frequency second rank rotational mode is roughly[24]

$$\tau \sim (fb^2/k_BT)N^{1+\delta} \quad (7)$$

where N is the number of bonds in the chain and δ is the excluded volume exponent (roughly $\delta = 1.2$).[70] The correlation time, τ_{zz}, corresponds to the slowest process observed in the present study, and, consequently, it is the most likely candidate for the application of eq (7) which predicts that

$$\tau_{zz}(C_{21})/\tau_{zz}(C_9) \simeq 7.5 \quad (8)$$

as compared to the corresponding experimental ratios of roughly 4 at 313 and 353 K. The Rouse model predications were based on the longest wavelength rotational mode and, accordingly, the correlation time ratio will be overestimated by eq 8. Correlation times dependent on local processes (i.e., isomerizations) will have a weaker N-dependence than eq 7, as is found in τ_{zz} as well as τ_{xx}, τ_{yy}, and τ_{xy}. Thus, it can only be concluded that the experimental correlation times are scaling reasonably with chain lengths and provide a challenging opportunity for future theoretical analysis.

Qualitatively, the arguments for the chain length dependence of the anisotropy can be seen by examining a molecular model of a chain. The zz orientational function, which is directed along the local chain backbone, should have the strongest dependence on the chain length, followed by the xx and yy components. This is because a local isomerization can relax the xx and yy functions, but the zz component remains relatively unaffected. Since the xy function is dephased by any motion, it can be expected to be relatively chain length independent. However, the results in Table II show that this is not the case experimentally. Instead, the anisotropy ratios are nearly the same for both C_9 and C_{21} and this deserves further study.

V. Concluding Remarks

The labeled hydrocarbons $C_4D_9{}^{13}CH_2C_4D_9$, $C_7D_{15}{}^{13}CH_2CD_3$, and $C_{10}D_{21}{}^{13}CH_2C_{10}D_{21}$ have been synthesized and the rotational correlation times of various $^{13}CH_2$ groups measured using NMR coupled relaxation techniques. Correlation times were obtained from the spectral densities using the methods of Fuson et al.[1] and do not have a dependence upon the selected theoretical model. The experimental rotational correlation times for nonane were compared with the same quantities determined using a Brownian dynamics algorithm. A BD model was chosen because of its simplicity and because it serves as a natural starting point upon which more sophicated theories of flexible chain dynamics can be compared. Pragmatically, BD has successfully accounted for other transport properties of alkanes,[49] while no other theoretical model has been compared carefully and systematically with experiment.

The results from BD and experiment on nonane agree in that the anisotropy is greater in the middle of nonane (at C-5) than it is at the terminal methylene (at C-2). Furthermore, the chain shows local prolate symmetric top behavior. The agreement of these two approaches is particularly good at room temperature and above, while the agreement deteriorates at lower temperatures. At 233 K, the anisotropies at the terminal and central methylenes are the same (within experimental error), whereas BD predicts less anisotropy at the chain ends. Furthermore, the experimental correlation times are less than the theoretical values by a factor of 2. The breakdown of the BD model at low temperature was attributed to the neglect of the frequency dependence of the shear viscosity and the chain character of the deuterated diglyme solvent. Both of the issues deserve further attention, and full molecular

(70) Yamakawa, H. "Modern Theory of Polymer Solution"; Harper and Row: New York, 1971.
(71) Grote, R. F.; Hynes, J. T. *J. Chem. Phys.* **1980**, *76*, 2715.
(72) Grote, R. F.; Vander Zwan, G.; Hynes, J. T. *J. Phys. Chem.* **1984**, *88*, 4676.
(73) Velsko, S. P.; Fleming, G. R. *Chem. Phys.* **1982**, *76*, 3553.
(74) Courtney, S. H.; Fleming, G. R. *Chem. Phys. Lett.* **1984**, *103*, 443.

dynamics calculations on neat alkanes are warranted.

The experimental rotational correlation times for the central methylene in heneicosane were greater, as expected, than those for the central methylene in nonane. However, contrary to intuition, the experimental anisotropies of the central methylenes in heneicosane and nonane were the same, and this issue deserves further attention.

The experimental techniques used here and the theory developed in the preceding paper demonstrate quite forcefully that NMR can be used to analyze the rotational dynamics of flexible molecules. The richness in information derived from these NMR methods (in principle these are four correlation times at each methylene in the chain) offers an unusually large amount of data for theoretical analysis. This provides justification for theoretical refinements not previously warranted owing to the paucity of experimental parameters. Furthermore, the experimental results may readily be placed in a form suitable for direct comparison to theory. Further coupled relaxation experiments could substantially improve our understanding of transport properties of flexible molecules. For example, it would be useful to investigate NMR coupled relaxation from smaller alkanes such as butane in simple solvents and to contrast the observed shear viscosity dependence with that from longer alkanes. This series of experiments could shed some light on the effective viscosity for combined internal and overall rotation. Also it would be valuable to understand how an imbedded electric dipole in an alkane affects reorientation and how the solvent (with and without a dipole moment) influences the correlation time through long-range interactions.

Acknowledgment. The Utah group is grateful to the National Institute of Health, Grant No. GM08521-24, for partial support of this research. G.T.E. is supported in part by a grant from the National Science Foundation and wishes to express his gratitude for the hospitality and guidance of Professor Daniel Kivelson during G.T.E.'s sabbatical leave at UCLA.

Appendix I

Air- and moisture-sensitive reactions were conducted in an oven-dried apparatus which was cooled in a stream of nitrogen or argon. THF was distilled from sodium under nitrogen just prior to use; ether was distilled from lithium aluminum hydride. Potassium [^{13}C]formate was dried at 0.01 mm and 52 °C for 24 h over calcium chloride. Acetonitrile was reagent grade stored over 4A sieves. Red phosphorus was well washed with water and dried overnight at 0.1 mm and 100 °C.

Diphenylmethyl [^{13}C]Formate (I). A solution of 0.66 g of 18-crown-6 and 4.96 g (59 mmol) of potassium [^{13}C]formate (90% ^{13}C; KOR Isotopes) in 32 mL of dry acetonitrile was stirred for 30 min; 13.23 g (53.3 mmol) of diphenylmethyl bromide (Aldrich redistilled, mp 36–42 °C) was then added and mixture refluxed for 48 h. After evaporation of the solvent, benzene was added and the solid salt was filtered and washed well with benzene. The product (I) (10.14 g, 47.8 mmol, 89.3%), boiled at 119.5–121 °C (0.3 mm); bp 104 °C is reported for the unlabeled compound.[75]

Benzyl [^{13}C]Formate (V). In like manner, 0.26 g of 18-crown-6 in 15 mL of acetonitrile with 1.9 g of potassium [^{13}C]formate was stirred for 30 min, after which 2.46 mL (20.7 mmol) of benzyl bromide (Fisher Scientific) was added dropwise; the mixture was refluxed using a heating mantle for 49 h. The solvent was evaporated and benzene was added. The solid salt was filtered and washed throughly with benzene. This treatment gave the product (V) (1.89 g, 13.8 mmol, 66.8%) which boiled at 82–84 °C (17 mm) was found to be pure by ^{1}H NMR.

5-Hydro-5-nonanol-*5*-^{13}C-d_{18} (II). Upon dropwise addition of 5 g (34.3 mmol) of perdeuteriobutyl bromide (Merck, 98 atom% D, previously dried over 3A sieves and removed by syringe) in 5 mL of THF to 0.84 g (35 mmol) of magnesium in 25 mL of THF at room temperature, the reaction started immediately. The addition was continued while the solution was brought to reflux, the bromide was rinsed in with four 1-mL portions of THF, and refluxing was maintained thereafter for 45 min. The solution was cooled lightly and 3.66 g (17.3 mmol) of diphenylmethyl [^{13}C]formate in 4 mL of THF was added dropwise while holding the solution at reflux. It was then refluxed for 75 min. While cooling in ice water, 2 mL of water was added followed by a solution of 1 mL of concentrated hydrochloric acid in 10 mL of water. After stirring for 15 min, the THF was distilled through a 10-cm Vigreux column and the aqueous part was saturated with sodium sulfate and extracted with ether. The dried ether extract (Na_2CO_3) was distilled to give 1.85 g (11.3 mmol, 66.1%) of II, bp 83–86 °C (10–11 mm); for the nonlabeled 5-nonanol, bp 97–98 °C (20 mm).[76]

5-Hydro-5-iodononane-*5*-^{13}C-d_{18} (III). The procedure is that of Prout.[77] To 1.76 g (10.8 mmol) of the above alcohol and 1.01 g (33 mmol) of red phosphorus, cooled to 4 °C, was added 4.1 g (16 mmol) of powdered iodine. This mixture was then stirred for 25.5 h at 4 °C while protected from moisture. After warming to room temperature, 10 g of ice was added and the mixture extracted with three 35-mL portions of ether. The ether was washed with aqueous sodium bisulfite and then with brine, dried (K_2CO_3), and distilled. The product (2.31 g, 8.52 mmol, 78.8%) boiled at 97–99 °C (13 mm) and was pure by ^{1}H and by ^{13}C NMR.

5,5-Dihydrononane-*5*-^{13}C-d_{18} (IV). The procedure followed is due to Krishnamurthy.[78,79] The iodo compound above (2.31 g) in 10 mL of THF was added to 17 mL of 1 M lithium triethylborohydride (17 mmol) in THF and the addition completed with 5 mL of THF. The solution was refluxed for 6 h, chilled in ice water, and decomposed with 10 mL of water followed by 10 mL of 6 N hydrochloric acid. The material was collected with 50 mL of pentane and 50 mL of brine and the aqueous part extracted with 50 mL of pentane. The organic portion was washed with 50-mL portions of calcium chloride (20 g per 100 mL) and dried (Na_2SO_4); the pentane was stripped off through a 10-cm Vigreux column. The middle portion boiled at 133–135 °C (0.8 g, 5.5 mmol, 64%) and was pure material (IV) by ^{1}H and ^{13}C NMR. Two NMR samples were made: one contained 0.0748 g of IV dissolved in 3.3204 g of perdeuteriodiglyme (2.22 mol %), and the other contained 0.0847 g of this nonane and 2.8629 of CD_2Cl_2 (1.77 mol %), both in 12-mm NMR tubes. The samples were subjected to five freeze–pump–thaw cycles to degas them, then sealed under vacuum. Carbon-13 and proton spectra showed these to be pure samples.

11-Hydro-11-heneicosanol-*11*-^{13}C-d_{42} (VI). Dropwise addition of 5 g of perdeuteriodecyl bromide (Merck, 98 atom % D) in 10 mL of ether to 0.51 g (0.021 g atom) of magnesium and several small crystals of iodine in 20 mL of ether at room temperature followed by stirring for 30 min gave the Grignard reagent. After addition of 1.42 g (10.8 mmol) of benzyl [^{13}C]formate (V) at room temperature and stirring overnight, the reaction mixture was decomposed with dilute sulfuric acid and collected in pentane. The residue left after evaporation of the pentane was heated on the steam bath for 3 h with 1.3 mL of 45% potassium hydroxide and 2 mL of water, diluted with water, chilled, filtered, and washed with ice water to yield compound VI (3.43 g, 9.66 mmol, 93.5%), mp 48–60 °C; mp 71.3–72.5 °C is reported for the natural abundance material.[80]

11-Hydro-11-iodoheneicosane-*11*-^{13}C-d_{42} (VII). Using the same procedure as described above for iodononane, 3.43 g of the carbinol with 1 g of phosphorus was combined with 4.05 g (15.9 mmol) of iodine and 10 mL of chloroform at 0 °C and stirred for 21 g at room temperature. The workup previously described gave 4.49 g (9.66 mmol, 100%) of VII.

11,11-Dihydroheneicosane-*11*-^{13}C-d_{42} (VIII). All of the above iodoheneicosane in 5 mL of THF was added with the aid of two 5-mL portions of THF to 20 mL (20 mmol) of 1 M lithium triethylborohydride; the solution was refluxed for 6 h. The workup described for IV gave 3.11 g (9.2 mmol, 95%) of VIII, a colorless waxy solid, mp 34–39 °C (the unlabeled compound melts at 40.2 °C).[81] The product contained no impurities as shown by ^{1}H and ^{13}C NMR. The NMR sample was made by placing 0.05249 g of this material and 2.5488 g of perdeuteriodiglyme in a 12-mm NMR tube. The sample was degassed using five freeze–pump–thaw cycles and sealed under vacuum, giving a sample composition of 8.28 mol %.

Octanonitrile-*1*-^{13}C-d_{15} (IX). Following a procedure previously described,[82] a suspension of 9.12 g (32.7 mmol) of silver tosylate in 90 mL of acetonitrile was chilled in an ice–water bath. To this was added dropwise 5.06 g (26.1 mmol) of perdeuterioheptyl bromide (KOR Isotopes, 97.7% enriched) with three 5-mL portions of acetonitrile to assist the transfer. The material was stirred for 22 h at room temperature. The

(75) Bunton, C. A.; Day, J. N. E.; Flowers, R. H.; Sheel, P.; Wood, J. L. *J. Chem. Soc.* **1957**, 963.

(76) Coleman, G. H.; Craig, D. "Organic Synthesis", Collect. Vol. II; Wiley: New York, 1943; p 179.

(77) Prout, F. S.; Cason, J.; Ingersoll, A. W. *J. Am. Chem. Soc.* **1948**, *70*, 298.

(78) Krishnamurthy, S.; Brown, H. C. *J. Org. Chem.* **1983**, *48*, 3089.

(79) Krishnamurthy, S.; Brown, H. C. *J. Org. Chem.* **1982**, *47*, 276.

(80) Breausch, F. L.; Sokullu, S. *Chem. Ber.* **1953**, *86*, 678.

(81) Schaerer, A. A.; Busso, C. J.; Skinner, L. B. *J. Am. Chem. Soc.* **1955**, *77*, 2017.

(82) Jacobs, T. L.; Macomber, R. S. *J. Am. Chem. Soc.* **1969**, *91*, 4824.

silver bromide was filtered and washed with acetonitrile; the filtrate was poured into 450 mL of water. The ether extract was washed with water and dried (Na_2SO_4–K_2CO_3). After removal of the ether, the residue was evacuated to 0.1 mm for 5 min. This residue in 21 mL of dimethyl sulfoxide was added dropwise to 1.76 g (26.6 mmol) of powdered potassium [^{13}C]cyanide (Prochem. 91% ^{31}C) in 18 mL of dimethyl sulfoxide held in a bath at 124–134 °C. The procedure is that of Friedman,[83] who used halides with potassium cyanide in DMSO. The bath was raised to 138–145 °C and stirring continued for 4 h. The mixture was then stirred at room temperature overnight. After addition to 95 mL of cold water and ether extraction, the extract was washed with water and dried (Na_2SO_4). Distillation gave 2.53 g of IX, bp 87–89 °C (18 mm) containing a small immiscible droplet. Redrying in a benzene solution (Na_2SO_4) and distillation gave 2.39 g (17 mmol, 65.1% over two steps), bp 85.5–87 °C (17 mm) still containing the immiscible droplet.

1-Hydrooctanal-*1*-^{13}C-d_{15} (X). The procedure of Keely[84] was used. A solution of 18 mL (18 mmol) of diisobutylaluminum hydride (Aldrich, 1 M in toluene) in 35 mL of ether was added slowly to 2.13 g (15.1 mmol) of the above cyanide in 20 mL of ether while stirring in a bath at 22 °C. After 45 min at 22 °C, the solution was refluxed gently for 30 min. The chilled solution was decomposed with 1.6 mL of water in 25 mL of dioxane, 25 mL of water was added, and the solution was shaken with 160 mL of 1 N hydrochloric acid. After 15 min standing the acid treatment was repeated. The ether extract was washed with 2% aqueous sodium carbonate and water and dried ($MgSO_4$). Distillation gave 1.68 g of X (11.7 mmol, 77.5%), bp 68–71 °C/(17 mm). About 13% of the starting cyanide (IX) was shown to be still present by ^{13}C NMR. This mixture was used in the next step without further purification.

2-Hydro-2-nonanol-*2*-^{13}C-d_{18} (XI). A stir bar and 0.15 g of Mg were placed in a dried, argon-flushed flask. A rubber septum was placed on top of the flask, and 15 mL of ether, freshly distilled from LiAlH, was added via syringe. The seal was broken on 5 g of ICD_3 (Merck) and 0.4 mL was delivered dropwise with the syringe. The mixture was cooled in an ice bath after the reaction started and stirred for 25 min after all of the iodomethane was added. An additional 0.15 mL of the perdeuterioiodomethane was added, the reaction mixture was stirred for 5 min, and then 0.05 mL more of the iodomethane was added and stirred for 10 min, until all of the Mg was used. While the mixture was cooled in the ice bath, the aldehyde from the previous step was added dropwise over 25 min using the syringe and stirred for 30 min at room temperature. The reaction mixture was cooled and 1 mL of water and then 3 mL of 0.2 N HCl are added. The mixture was extracted with ether, washed with aqueous sodium bisulfite and with water, and dried overnight (Na_2SO_4); the ether was evaporated. Because of the small quantity of XI obtained (about 0.6 g), distillation was not attempted.

2-Hydro-2-iodonanane-*2*-^{13}C-d_{18} (XII). The same procedure as given above for the 5-iodononane (III) and the iodoheneicosane (VII) was followed, using 0.37 g (12 mmol) of phosphorus and 1.54 g (6.1 mmol) of I_2 in 15 mL of clean dry chloroform. No distillation was attempted and this material (XII) was used in the next step.

2,2-Dihydrononane-*2*-^{13}C-d_{18} (XIII). The same procedure described above for IV was followed, using 0.45 g (1.65 mmol) of the above iodo compound (XII) with 3.5 mL of 1 N lithium triethylborohydride in THF. Here again, no distillation was attempted, and the final yield was approximately 0.2 g (1.4 mmol, 82%) of compound XIII. To make the NMR sample, 0.1678 g of this material was weighed into a 12-mm NMR tube along with 2.1831 g of perdeuteriodiglyme, giving a sample composition of 7.74 mol %. The sample was subjected to five freeze–pump–thaw cycles and sealed under vacuum. The ^{13}C spectrum reveals the expected 1:2:1 triplet with small peaks on the downfield side of each component in the triplet, also with intensity 1:2:1. These low-intensity lines are attributed to the presence of a proton adjacent to the $^{13}CH_2$ group in some of the sample molecules, causing a small isotope shift. The amount of sample labeled in this way is difficult to determine owing to the broad line (5 Hz) and small shifts involved, but was less than 10%. There was no simple way to separate these isotopic isomers. Since the *minimum* proton–proton distance between protons on adjacent carbons is only 1.5 Å, this minor isotopic impurity does not significantly alter the relaxation results. Fortunately, in all relaxation experiments performed on this sample, the isotopically shifted lines track the unshifted major lines. The ^{13}C spectrum also initially revealed a doublet with a temperature-dependent chemical shift due to the presence of unreacted iodononane (present to less than 10% of the labeled nonane). At 313 K the upfield component of the doublet overlapped the downfield component of the triplet. Accordingly, this sample was broken open and the nonane and diglyme were codistilled to eliminate the iodo impurity, then again placed in a 12 mm NMR tube, degassed as before, and sealed under vacuum. This sample was used for the relaxation studies.

(83) Friedman, L.; Schechter, H. *J. Org. Chem.* **1960**, *25*, 877.
(84) Keely, S. L.; Tahk, F. C. *J. Am. Chem. Soc.* **1968**, *90*, 5584.

Registry No. I, 98195-33-6; II, 98195-35-8; III, 98195-37-0; IV, 98195-30-3; V, 98195-34-7; VI, 98195-38-1; VII, 98195-40-5; VIII, 98195-32-5; IX, 98195-41-6; X, 98195-43-8; XI, 98195-44-9; XII, 98195-45-0; XIII, 98195-31-4; $H^{13}C(O)OK$, 86967-49-9; Ph_2CHBr, 776-74-9; $PhCH_2Br$, 100-39-0; $CD_3(CD_2)_3Br$, 98195-36-9; $CD_3(CD_2)_9Br$, 98195-39-2; AgOTs, 16836-95-6; $CD_3(CD_2)_6Br$, 98195-42-7; ICD_3, 865-50-9.

Communications to the Editor

Spontaneous Fragmentation of Cationic Polystyrene Chains

A. Grey Craig and Peter J. Derrick*

School of Chemistry, University of New South Wales
Kensington, N.S.W., Australia

Received May 22, 1985

Using mass spectroscopic techniques, we have found that at low energies cationic polystyrene chains $[M]^{+\cdot}$ (in the mass range 500–4500 units) fragment at bonds near the ends of chains. Bonds in the middle of the chains tend not to rupture. The effect is most pronounced with the longest chains. This preference for fragmentation near the ends of chains is proposed to be a consequence of stabilization of larger fragment ions due to charge delocalization. Polybutadiene $[M]^{+\cdot}$, polyethylene glycol $[M + H]^+$, and polypropylene glycol $[M + H]^+$ cations behave similarly.[1]

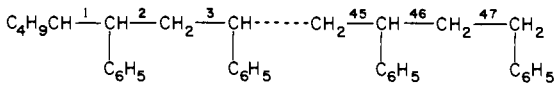

(1)

Polystyrene molecular ions $[M]^{+\cdot}$ were formed by field desorption,[2-4] and their fragmentation studied by mass-analyzed ion kinetic energy (MIKE) spectroscopy.[5,6] The MIKE spectrum of a given $[M]^{+\cdot}$ was observed above a characteristic emitter

(1) Craig, A. G.; Derrick, P. J., unpublished results.
(2) Beckey, H. D. "Principles of Field Ionization and Field Desorption Mass Spectrometry"; Pergamon: London, 1977.
(3) (a) Neumann, G. M.; Cullis, P. G.; Derrick, P. J. *Z. Naturforsch. A* **1980**, *35*, 1090. (b) Craig, A. G.; Cullis, P. G.; Derrick, P. J. *Int. J. Mass Spectrom. Ion Phys.* **1981**, *38*, 297.
(4) (a) Lattimer, R. P.; Harmon, D. J.; Welch, K. R. *Anal. Chem.* **1979**, *51*, 1293. (b) Matsuo, T.; Matsuda, H.; Katakuse, I. *Anal. Chem.* **1979**, *51*, 1329. (c) Matsuo, T.; Matsuda, H.; Katakuse, I. *Adv. Mass Spectrom.* **1980**, *8*, 990. (d) Lattimer, R. P.; Harmon, D. J.; Hansen, G. E. *Anal. Chem.* **1980**, *52*, 1808. (e) Lattimer, R. P.; Hansen, G. E. *Macromolecules* **1981**, *14*, 776. (f) Lattimer, R. P.; Schulten, H.-R. *Int. J. Mass Spectrom. Ion Phys.* **1983**, *52*, 105.
(5) (a) Cooks, R. G.; Beynon, J. H.; Caprioli, R. M.; Lesier, G. R. "Metastable Ions"; Elsevier Scientific Publishing Co.: Amsterdam, 1973. (b) "Tandem Mass Spectrometry"; ed. McLafferty, F. W., Ed.; Wiley: New York, 1983.
(6) (a) Darcy, M. G.; Rogers, D. E.; Derrick, P. J. *Int. J. Mass Spectrom. Ion Phys.* **1978**, *27*, 335. (b) Cullis, P. G.; Neumann, G. M.; Rogers, D. E.; Derrick, P. J. *Adv. Mass Spectrom.* **1980**, *8*, 1729.

0002-7863/85/1507-6707$01.50/0